

ARTICLES

Time-Dependent Radiolytic Yields of the Solvated Electrons in 1,2-Ethanediol, 1,2-Propanediol, and 1,3-Propanediol from Picosecond to Microsecond**Mingzhang Lin,[†] Mehran Mostafavi,^{*‡} Yusa Muroya,[§] Zhenhui Han,[†] Isabelle Lampre,[‡] and Yosuke Katsumura^{†,§,||}**

Department of Nuclear Engineering and Management, School of Engineering, The University of Tokyo, Hongo 7-3-1, Bunkyo-ku, Tokyo 113-8656, Japan, Laboratoire de Chimie Physique/ELYSE, UMR 8000 CNRS/Université Paris-Sud, Centre d'Orsay, Bât. 349, 91405 Orsay Cedex, France, and Nuclear Professional School, School of Engineering, The University of Tokyo, 2-22 Shirakata Shirane, Tokaimura, Nakagun, Ibaraki 319-1188, Japan

Received: June 16, 2006; In Final Form: August 15, 2006

The absorption spectra of the solvated electron in 1,2-ethanediol (12ED), 1,2-propanediol (12PD), and 1,3-propanediol (13PD) have been determined by nanosecond pulse radiolysis techniques. The maximum of the absorption band located at 570, 565, and 575 nm for these three solvents, respectively. With 4,4'-bipyridine (44Bpy) as a scavenger, the molar extinction coefficients at the absorption maximum of the solvated electron spectrum have been evaluated to be 900, 970, and 1000 mol⁻¹ m² for 12ED, 12PD, and 13PD, respectively. These values are two-thirds or three-fourths of the value usually reported in the literature. With these extinction coefficients, picosecond pulse radiolysis studies have allowed us to depict the radiolytic yield of the solvated electron in these solvents as a function of time from picosecond to microsecond. The radiolytic yield in these viscous solvents is found to be strongly different from that of water solution.

Introduction

The chemical effects of ionizing radiation on liquids have been extensively studied for decades in steady state and pulse regimes. Among the radicals produced by irradiation, the solvated electron (e_s⁻) has been the subject of a huge amount of publications. Since the first measurements in water, the optical absorption of the solvated electron has been observed in more than 100 solvents. Thanks to that property, the reactivity of the solvated electron has been studied by transient absorption measurements in many solvents, such as water or alcohols, using pulse radiolysis techniques.^{1–8}

Recently, we investigated the influence of temperature on the absorption spectrum of the solvated electron in a wide range of temperature in several polyalcohols, 1,2-ethanediol (12ED), 1,2-propanediol (12PD), and 1,3-propanediol (13PD).^{9,10} We also studied the dynamics of the electron solvation in these viscous solvents by femtosecond laser spectroscopy.^{11–13} In the literature, we found some discrepancies in the values of the radiolytic yield and the extinction coefficient of the solvated electron in these solvents.

Indeed, the transient optical spectrum of electrons solvated in 1,2-ethanediol was determined by nanosecond pulse radiolysis studies^{6,14–16} and by femtosecond photodetachment experiments with iodide.¹⁷ At 298 K, the maximum of the absorption band is located at about 570 nm, which corresponds to a transition energy $E_{\text{max}} = 2.18$ eV. In comparison with those in other polar solvents, that transition energy, like those obtained for the other diols, is rather high and just below the value in glycerol (2.31 eV).^{6,15,18} The extinction coefficient at the maximum of the absorption band is reported to be $\epsilon_{\text{max}}(\text{e}_s^-) = 1.4 \times 10^3$ mol⁻¹ m².^{14,19,20} The value of the extinction coefficient at maximum reported by Sauer et al. is based on a radiation chemical yield (called G value) after spur reactions for e_s⁻, (G_{fi}), of 0.12 μ mol J⁻¹.¹⁴ Jou and Freeman later confirmed that the product of ϵ_{max} by G_{fi} in 1,2-ethanediol was around 1.8×10^{-3} m²/J.¹⁸ However, in comparison with the radiolytic yield after spur reaction determined in other solvents such as methanol or ethanol (where G_{fi} is around 0.21 μ mol J⁻¹ or slightly less), the e_s⁻ yield of 0.12 μ mol J⁻¹ in 12ED reported by Sauer et al.¹⁴ is clearly lower. Similarly, the optical absorption spectrum of the solvated electron in 1,2-propanediol and 1,3-propanediol was recorded by nanosecond pulse radiolysis measurements, and the value of $G_{\text{fi}}\epsilon_{\text{max}}(\text{e}_s^-)$ at the maximum of the absorption band was determined to be around 1.15×10^{-4} m²/J in both solvents as in 12ED.¹⁶ Using a correlation between the value of G_{fi} and the static electric constant of the alcohols, Jay-Gerin and Ferradini calculated the values of G_{fi} and $\epsilon_{\text{max}}(\text{e}_s^-)$ for the polyols.²¹ The value of $\epsilon_{\text{max}}(\text{e}_s^-)$ at the maximum of the absorp-

* Address correspondence to this author at Laboratoire de Chimie Physique/ELYSE, UMR 8000 CNRS/Université Paris-Sud, Centre d'Orsay, Bât. 349, 91405 Orsay Cedex, France.

[†] Department of Nuclear Engineering and Management, University of Tokyo.

[‡] UMR 8000 CNRS/Université Paris-Sud.

[§] Nuclear Professional School, The University of Tokyo.

^{||} Department of Nuclear Engineering and Management, School of Engineering, The University of Tokyo, Hongo 7-3-1, Bunkyo-ku, Tokyo 113-8656, Japan. Fax/telephone: +81-3-5841-8624. E-mail: katsu@n.t.u-tokyo.ac.jp.

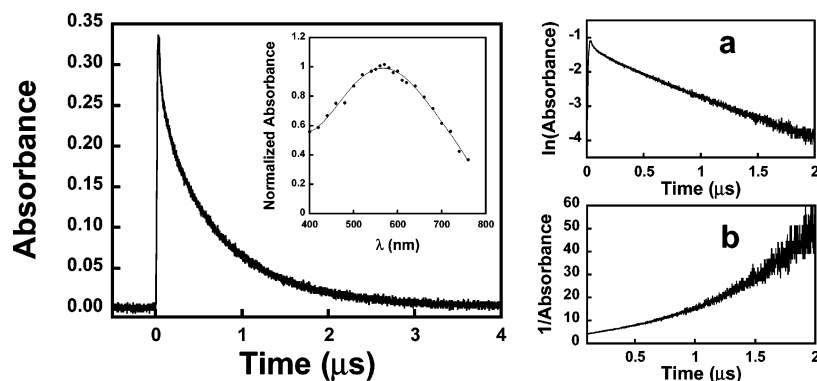


Figure 1. Left: decay of the solvated electron in pure 12ED monitored at 570 nm. Inset: Normalized absorption spectrum of the solvated electron in pure 12ED measured just at the end of pulse (pulse duration: 20 ns). Right: (a) first-order and (b) second-order treatment of the decay.

tion band was estimated to be 800, 750, and 650 mol⁻¹ m² for 12ED, 12PD, and 13PD, respectively.²²

In that context, we undertook pulse radiolysis studies in order to determine the extinction coefficients and the time-dependent radiolytic yield of the solvated electron in these dialcohols. For the first purpose, we used 4,4'-bipyridine as a scavenger of the solvated electron, because of its excellent solubility, its high reactivity toward the solvated electron, as well as its fairly stable electron adducts. Then, knowing the extinction coefficient, thanks to kinetic signals obtained by the recently constructed picosecond pulse radiolysis system,^{23–25} we describe the time-dependent radiolytic yields of the solvated electron in these diols from the picosecond to the microsecond time range.

Experimental Section

1,2-ethanediol (12ED, ethylene glycol), 1,2-propanediol (12PD, propylene glycol), 1,3-propanediol (13PD), as well as 4,4'-bipyridine (44Bpy) and methyl viologen (MV²⁺) were purchased from Wako Pure Chemical Industries, Ltd., and used as received. The sample solutions were freshly prepared, deaerated by Ar gas for about 15 min, and then continuously purged with Ar gas above the surface during the measurements. Due to the low volatility of these diols, the mass loss was negligible. The solubility of 44Bpy is limited in 12ED, and we could not use a higher concentration than 0.2 M.

The nanosecond pulse radiolysis experiments were carried out at the University of Tokyo using a linear electron accelerator (energy, 35 MeV; pulse width, 10 ns) coupled with an absorption spectroscopic detection system. The trigger signals to the accelerator and the Xe pulse lamps, the change in the monochromator wavelength, as well as the data transfer from the oscilloscope were controlled by PCs through GPIB. Each acquisition had 10 000 data points. A blocking filter at 340 nm was used to cut the scattered and multiple-orders light for the wavelength range 340–520 nm, while a filter at 520 nm was used for wavelength range 520–900 nm. The optical path length of the quartz cell was usually 20 mm. The dosimetry was done with an N₂O-saturated 10 mM KSCN aqueous solution, taking $G\epsilon((\text{SCN})_2^{\bullet-}) = 5.2 \times 10^{-4}$ m²/J at 475 nm.²⁶ Then, the absorbed dose, *D*, in the alcohols was calculated by the equation $D_{\text{diol}} = D_{\text{H}_2\text{O}} \times \rho_{\text{diol}}$, where ρ_{diol} stands for the density of the diol. The dose fluctuations were less than 5% during a day-long experiment.

Picosecond pulse radiolysis measurements were performed with a pulse-and-probe method using the same facility. Details and performance of the system have been reported elsewhere.^{23–25} Briefly, an S-band linear accelerator with a laser photocathode rf gun was operated at a repetition rate of 10 Hz. A femtosecond

Ti:sapphire laser beam (795 nm) was split by a half-mirror into two equal pulses and used as a probe-analyzing light after passing through a quartz cell filled with D₂O for generating a white-light continuum and as an injector for the photocathode rf gun after third-harmonic generation in β-barium borate (BBO) crystals. An electron beam with a pulse duration of 3 ps (fwhm), a charge of 1 nC, and an energy of 20 MeV was produced as an irradiation source. The electron beam and the femtosecond laser are synchronized within 2 ps (root-mean-square value), and an optical delay stage was employed to change the time interval between the electron pulse and the probe light pulse. The signal intensities were measured using Si PIN photodiodes (Hamamatsu, S1722-02) and an oscilloscope (Hewlett-Packard, HP54845). The optical path length of the quartz cell was usually 10 mm. For measurements of $G(e_s^-)\epsilon(e_s^-)$ in the alcohols, first, a kinetic signal of the hydrated electron at 700 nm in pure water was recorded

$$A(e_{\text{aq}}^-) = \epsilon(e_{\text{aq}}^-) \times l \times c = \epsilon(e_{\text{aq}}^-) \times l \times G(e_{\text{aq}}^-) \times D_{\text{H}_2\text{O}} \quad (1)$$

where $A(e_{\text{aq}}^-)$ is the absorbance of the hydrated electron, $\epsilon(e_{\text{aq}}^-)$ is the extinction coefficient, *l* is the optical path length of the cell, *c* is the concentration of hydrated electron, $G(e_{\text{aq}}^-)$ is the radiolytic yield of the hydrated electron, and $D_{\text{H}_2\text{O}}$ represents the dose per pulse in water. Second, under the same experimental conditions, the kinetic signal of the solvated electron (at the absorption band maximum) in an alcohol was measured

$$A(e_s^-) = \epsilon(e_s^-) \times l \times c = \epsilon(e_s^-) \times l \times G(e_s^-) \times D_{\text{H}_2\text{O}} \times \rho_{\text{diol}} \quad (2)$$

where ρ_{diol} is the density of alcohol.

Therefore, at a given time, we have

$$G(e_s^-)\epsilon(e_s^-) = G(e_{\text{aq}}^-) \times \epsilon(e_{\text{aq}}^-) \times A(e_s^-) / [A(e_{\text{aq}}^-) \times \rho_{\text{diol}}] \quad (3)$$

Since $G(e_{\text{aq}}^-)\epsilon(e_{\text{aq}}^-)$ has been well-established,²⁷ from the above equation we may obtain $G(e_s^-)\epsilon(e_s^-)$ for the alcohols.

Results and Discussion

Figure 1 shows the time profile of the solvated electron in pure 12ED solution obtained by nanosecond pulse radiolysis (left). The decay at short times is very fast. It is interesting to note that the decay follows a second-order law at short times and a first-order law at longer times (right). Due to the high

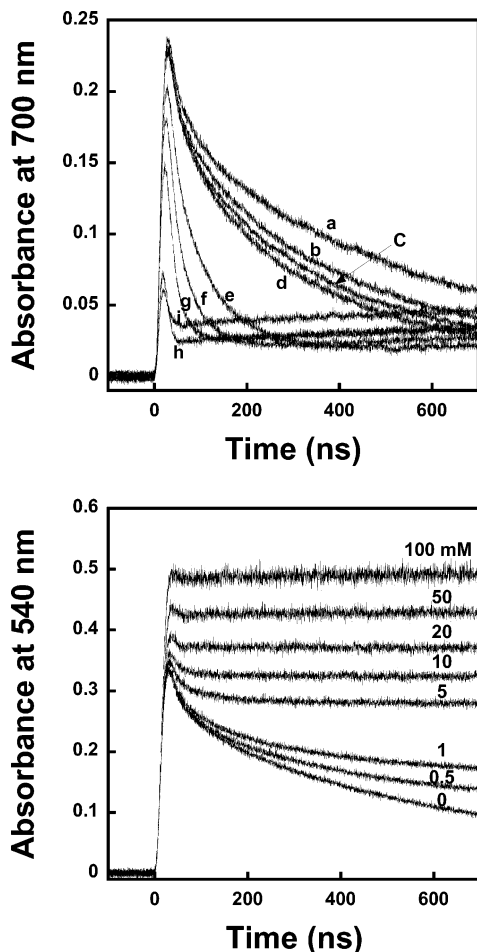


Figure 2. Time profiles at 700 nm (top) and at 540 nm (bottom) obtained by pulse radiolysis of 12ED solutions in the presence of different concentrations of 44Bpy: (a) pure 12ED, and (b) 0.5, (c) 0.75, (d) 1, (e) 5, (f) 10, (g) 20, (h) 50, and (i) 100 mM 44Bpy.

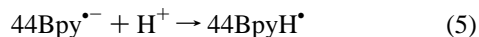
viscosity of 12ED, the spur reactions are slow. Within the first 300 ns, the strong decay is primarily due to the spur reactions. This behavior is very different from that of the hydrated electron. The inset of Figure 1 (left) shows the absorption spectrum of the solvated electron in pure 12ED.

Different concentrations of 44Bpy from 0.5 mM up to 100 mM are used to scavenge the solvated electron. The kinetics are observed at 700 and 540 nm (Figure 2). The kinetics observed at 700 nm are mainly due to the solvated electron, although for the high concentrations of scavenger (20, 50, and 100 mM), a slow increase of the absorbance is observed at longer times.

The decay of the solvated electron is accelerated by increasing the concentration of the scavenger due to the following reaction:



The anion $\text{Bpy}^{\bullet-}$ reacts very quickly with H^+ to form the neutral radical BpyH^\bullet .



The maximum of the absorption band of this neutral radical is located at 540 nm,²⁸ and the extinction coefficient in aqueous solution is known to be $1300 \text{ mol}^{-1} \text{ m}^2$.²⁹

Both the solvated electron and the electron adduct of 44Bpy absorb at 540 nm. So, at 540 nm, at short times, the absorption just after the pulse is due to the solvated electron, while at longer

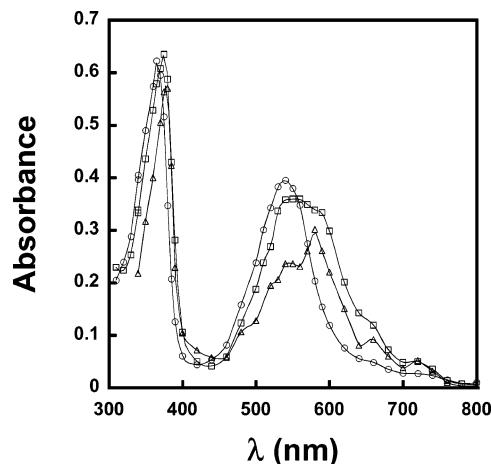
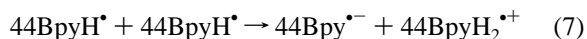


Figure 3. Transient absorption spectra obtained by pulse radiolysis of a 12ED solution containing 20 mM 44Bpy: (○) 300 ns, (□) 5 μs , and (△) 80 μs .

times, the absorption is related to 44BpyH^\bullet formed through reaction 5, which is stable for a few microseconds.

Figure 3 shows the transient absorption spectra obtained by pulse radiolysis of a 12ED solution containing 20 mM 44Bpy, and recorded at 300 ns, 5 μs , and 80 μs after the pulse. Only the characteristic absorption of 44BpyH^\bullet is observed shortly after the electron beam, but at longer times, the absorbance at 540 nm decreases and a new absorption peak appears at 580 nm, while the absorption peak in the spectral UV region shifts from 365 to 380 nm. The absorption bands at 380 and 580 nm could be assigned to the anion $44\text{Bpy}^{\bullet-}$ ^{30,31} or to the *N,N'*-dihydro radical cation $44\text{BpyH}_2^{\bullet+}$.³² In fact, the protonation or disproportionation reactions of 44BpyH^\bullet occur as in the reactions below³³



However, as $44\text{Bpy}^{\bullet-}$ produced in reaction 7 must be quickly protonated, the increase in the transient absorbance observed around 580 nm at longer times is attributed to the formation of $44\text{BpyH}_2^{\bullet+}$.

As shown in Figure 2, up to 600 ns, the change in the absorption spectrum does not affect the kinetics at 540 nm, even in a solution containing 100 mM 44Bpy. Even if the extinction coefficient of $44\text{BpyH}_2^{\bullet+}$ at 540 nm is higher than that of 44BpyH^\bullet , the signal is fairly flat without noticeable increase. From the kinetics (at 700 nm) at low concentrations (0–10 mM), we deduce the rate constant of reaction 4, taking into account the residual absorbance at the end of the decay of solvated electrons, which is due to the $44\text{BpyH}_2^{\bullet+}$. In Figure 4, the observed pseudo-first-order rate constant of the reaction is plotted as a function of the scavenger concentrations. From the slope of the curve, the rate constant of reaction 4 is obtained as $1.3 \times 10^9 \text{ dm}^3 \text{ mol}^{-1} \text{ s}^{-1}$. In similar conditions, the rate constant of the reaction of the solvated electron with MV^{2+} is determined to be $3.4 \times 10^9 \text{ dm}^3 \text{ mol}^{-1} \text{ s}^{-1}$ (Figure 4 and Table 1). The difference between these values is mostly due to the charge effect, since in 12ED, the charges are not fully screened by the solvent. The reported rate constant value of the reaction between the silver ion and the solvated electron in that solvent ($2.8 \times 10^9 \text{ dm}^3 \text{ mol}^{-1} \text{ s}^{-1}$)³⁴ is also in agreement with the above values in the case of diffusion-controlled reactions. In fact, the rate constant of a reaction between the solvated electron and a solute

TABLE 1: Properties and Results Obtained for the Three Diols and Water

S	$k(e_s^- + S)$ ($\text{dm}^3 \text{mol}^{-1} \text{s}^{-1}$)	$\eta^{25^\circ\text{C}}$ (mPa s)	dielectric constant	λ_{max} of e_s^- (nm)	ϵ ($\text{mol}^{-1} \text{m}^2$)	G ($\mu\text{mol J}^{-1}$)	G at 200 ns ($\mu\text{mol J}^{-1}$)
				12ED			
MV ²⁺	3.4×10^9	16.1	41.4	570	900 ± 50	0.43 (at 30 ps)	0.17
Ag ⁺	2.8×10^9 ^a	16.1	41.4	570	900 ± 50	0.43 (at 30 ps)	0.17
Bpy	1.3×10^9	16.1	41.4	570	900 ± 50	0.43 (at 30 ps)	0.17
				12PD			
Bpy	6.4×10^8	40.4	27.5	565	970 ± 50	0.35 (at 100 ps) ^b	0.17
				13PD			
Bpy	6.7×10^8	39.4	35.1	575	1000 ± 50	0.38 (at 100 ps) ^b	0.22
				Water			
Bpy	2.9×10^{10} ^c	0.89	78.4	720	1800	0.44 (at 30ps)	0.27

^a From ref 34. ^b A clear formation process of the solvated electron was found within about 50 ps. ^c From ref 48.

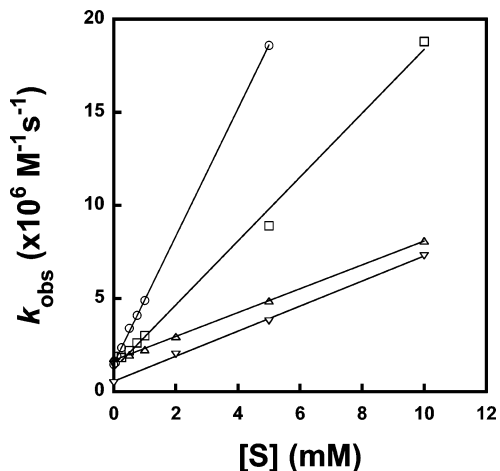


Figure 4. Observed rate constants of the reaction of the solvated electron with methyl viologen in 12ED (○), with 44Bpy in 12ED (□), in 12PD (△), and in 13PD (▽) as a function of the scavenger concentration [S].

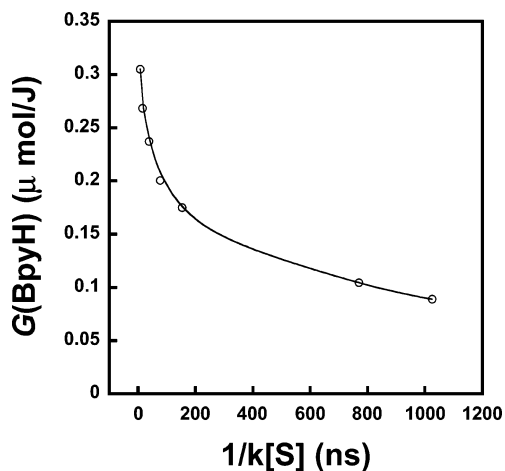


Figure 5. Formation yield of BpyH[•] as a function of the scavenging power in 12ED.

in an alcohol can depend strongly upon the electron solvation energy (trap depth) and on the liquid viscosity η .³⁵

From the plateau observed at 540 nm (Figure 2), for a given quencher concentration, by assuming an extinction coefficient of $1300 \text{ mol}^{-1} \text{ m}^2$ for 44BpyH[•] as in aqueous solutions,²⁹ we can obtain the concentration of 44BpyH[•] formed after the pulse. Figure 5 gives the formation yield of 44BpyH[•] versus the scavenging power. That yield of 44BpyH[•] corresponds to the yield of scavenged solvated electrons. According to the previous studies on the reactions of electrons with concentrated scavengers by picosecond pulse radiolysis, the scavenger can also react

either through static quenching or through reactions of the precursor of solvated electron.^{36–40} Experimentally, the yield of the solvated electron is decreased in the presence of a high concentration of scavengers, and the concentration at which the yield of the solvated electron decreases to 37% of its initial yield (without scavenger) is defined as C_{37} . For acetone and carbon tetrachloride in ethanol, the C_{37} values are 0.3 and 0.14 M, respectively.³⁷ Their C_{37} values in 12ED are about 3 times higher than in ethanol, that is, 1.0 and 0.36 M, respectively. There is no literature data for C_{37} of 44Bpy in 12ED. However, let us consider biphenyl, whose C_{37} in ethanol is 0.19 M;³⁷ then, in 12ED, its C_{37} would be about 0.6 M. From the similarity of the molecular structures, we suggest that C_{37} of 44Bpy in 12ED should also be about 0.6 M. In our experiments, the highest concentration of 44Bpy is 0.1 M, and this concentration might not result in significant reaction with the precursor to solvated electron.

At a concentration of 100 mM, almost all solvated electrons produced by the pulse are scavenged by 44Bpy. Therefore, we can deduce the extinction coefficient of the solvated electron. In fact, the absorbance at 540 nm (at time zero) in the absence and in the presence of 100 mM 44Bpy is 0.32 and 0.49, respectively.

According to the Beer–Lambert’s law, we have

$$\epsilon(e_s^- \text{ at } 540 \text{ nm})/\epsilon(44\text{BpyH}^\bullet \text{ at } 540 \text{ nm}) = A_{540\text{nm}}(0 \text{ mM})/A_{540\text{nm}}(100 \text{ mM}) \quad (8)$$

then

$$\epsilon(e_s^- \text{ at } 540 \text{ nm}) = 1300 \times 0.32/0.49 = 850 \text{ mol}^{-1} \text{ m}^2 \quad (9)$$

and because

$$\epsilon(e_s^- \text{ at } 540 \text{ nm})/\epsilon(e_s^- \text{ at } 575 \text{ nm}) = 0.97 \quad (10)$$

we obtain

$$\epsilon(e_s^- \text{ at } 570 \text{ nm}) = 880 \text{ mol}^{-1} \text{ m}^2 \quad (11)$$

We notice that, if the presolvated electron is scavenged by 44Bpy, the value $880 \text{ mol}^{-1} \text{ m}^2$ should be corrected to a lower value. But, as we reported above, we neglected the scavenging of the presolvated electron by 44Bpy. We may also estimate the $\epsilon(e_s^- \text{ at } 570 \text{ nm})$ from the time profile of the solvated electron in pure 12ED. In this measurement, the dose per pulse measured using 10 mM KSCN is 63 Gy. The absorbance in a 2 cm cell at 540 nm at the end of the pulse in the absence of scavenger is 0.32. A rough estimation of the radiolytic yield of the solvated electron can be deduced from the curve in Figure

5: $G(e_s^-)$ at the end of the pulse (~ 10 ns) is about $0.28 \mu\text{mol J}^{-1}$. From the following relation

$$A_{540\text{nm}}(10 \text{ ns}) = \epsilon(e_s^- \text{ at } 540 \text{ nm}) \times l \times c = \epsilon(e_s^- \text{ at } 540 \text{ nm}) \times l \times G(e_s^- \text{ at } 10 \text{ ns}) \times D_{\text{diol}} \quad (12)$$

we deduce the value of the extinction coefficient

$$\epsilon(e_s^- \text{ at } 540 \text{ nm}) = A_{540\text{nm}}(10 \text{ ns})/[l \times G(e_s^- \text{ at } 10 \text{ ns}) \times D_{\text{diol}}] = 910 \text{ mol}^{-1} \text{ m}^2 \quad (13)$$

Within the errors, the values obtained by the two different methods are in good agreement. Therefore, we can assume that the extinction coefficient at the maximum of the absorption band is

$$\epsilon(e_s^- \text{ at } 570 \text{ nm}) = 900 \pm 50 \text{ mol}^{-1} \text{ m}^2 \quad (14)$$

If we assume that the scavenging of presolvated electron by 44Bpy is negligible, the uncertainties regarding this estimation are mainly due to the fluctuations of the dose per pulse and to the error in the value of the extinction coefficient of BpyH[•]. With a similar procedure, we determine the rate constant of the solvated electron scavenging by 44Bpy (Figure 4) and the extinction coefficients of the solvated electron in 12PD and 13PD. The results are summarized in Table 1. The extinction coefficients of the solvated electron in these three solvents are 900, 970, and 1000 mol⁻¹ m² for 12ED, 12PD, and 13PD, respectively. These values are smaller than the reported value, 1400 mol⁻¹ m² for e_s⁻ in 12ED,¹⁴ but slightly higher than those proposed by Jay-Gerin et al.,²² which are 800, 750, and 650 mol⁻¹ m² for 12ED, 12PD, and 13PD, respectively. In the work of Sauer et al.,¹⁴ the biphenyl was used as the solvated electron scavenger, and $G_{\text{fi}}(e_s^- \text{ in ethanol}) = 0.1 \mu\text{mol J}^{-1}$ was taken as the reference standard for the determination of the extinction coefficient. However, nowadays, $G_{\text{fi}}(e_s^- \text{ in ethanol})$ is generally accepted to be $0.18 \mu\text{mol J}^{-1}$.⁴¹⁻⁴³ The lower value $G(e_s^-)$ might be due to the use of impure ethanol or high irradiation dose.⁴³ Then, if we take $G(e_s^- \text{ in ethanol}) = 0.18 \mu\text{mol J}^{-1}$ as the reference standard, ϵ for the solvated electron in 12ED would be around 820 mol⁻¹ m², which is in agreement with our result.

According to the literature, in 12ED at the wavelength of 570 nm, there is no solvation dynamics effect after 30 ps, and the kinetics observed at this wavelength is only due to the spur reactions.¹² Figure 6 (top) shows $G(e_s^-)$ in 12ED as a function of time from about 30 ps to 1 μs . There are two parts: curve a obtained by picosecond pulse radiolysis and curve b recorded by conventional nanosecond pulse radiolysis. As mentioned above, for picosecond pulse radiolysis, we have used, as the reference standard to calculate $G(e_s^-)\epsilon(e_s^-)$ in 12ED, the value $G(e_{\text{aq}}^-)\epsilon(e_{\text{aq}}^-) = 7.96 \times 10^{-4} \text{ dm}^3 \text{ J}^{-1}$ determined in water at 700 nm just after the pulse. Although two different independent methods are used and the measurements cannot cover all time regions (no data from 1 ns to a few tens of nanoseconds), it seems that curves a and b match each other well. For comparison, we also plot (Figure 6, curve d) the data obtained for the hydrated electron in previous work.²⁷ We observe that, at subnanosecond time range, the radiolytic yield of the solvated electron in 12ED and in water are very close, but at a longer time range, the yield of solvated electron in 12ED is much lower than in water. The yield of the solvated electron in 12ED, which is about $0.36 \mu\text{mol J}^{-1}$ at 1 ns, decreases strongly to the value of $0.17 \mu\text{mol J}^{-1}$ at 200 ns. In the case of water, for the same time range the yield changes from 0.37 to $0.27 \mu\text{mol J}^{-1}$. That

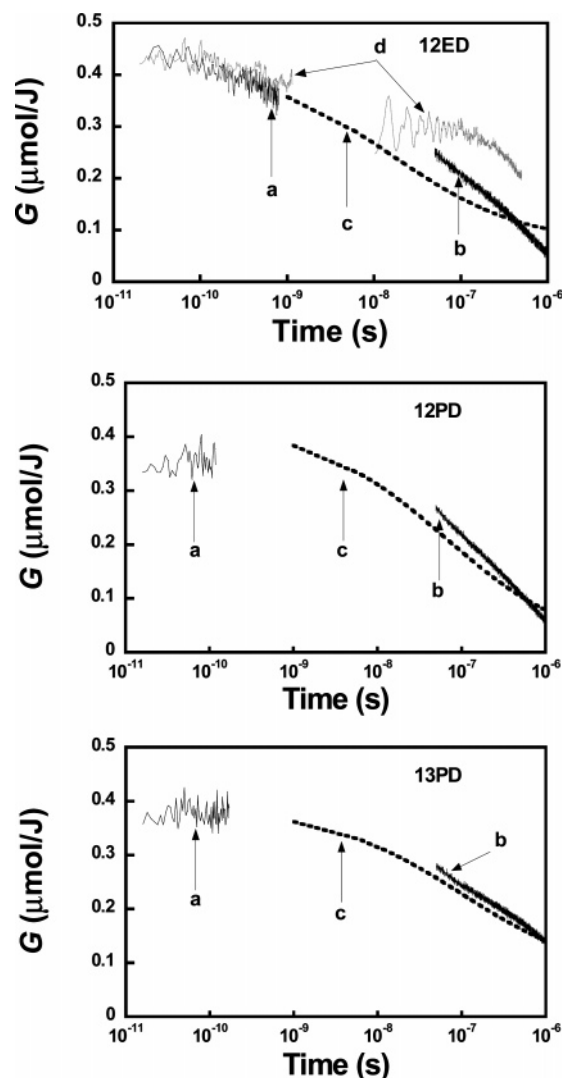


Figure 6. Time dependence of the radiolytic yield of the solvated electron in 12ED (top), in 12PD (middle), and in 13PD (bottom). (a) Picosecond pulse radiolysis measurements; (b) nanosecond pulse radiolysis studies; (c) calculation results of eq 18, which is the ILT of eq 16; (d) time-dependent G value of the hydrated electron reported in previous work.²⁷

means that the decay of the solvated electron through the spur reactions is more efficient in 12ED than in water. As the escape from spur reactions is dependent on the diffusion constant (inverse of viscosity) and as the spur reactions are not all diffusion-controlled, the high viscosity of solvents like diols partially prohibits the escape of solvated electrons from the spur reactions. Moreover, it is to be remembered that in alcohols the solvated electron can react with the solvent following a pseudo-first-order reaction⁴⁴



In the case of methanol, the rate constant of reaction 15 has been reported to be 8.5×10^3 ⁴⁵ or $1.1 \times 10^4 \text{ dm}^3 \text{ mol}^{-1} \text{ s}^{-1}$,⁴⁶ while for ethanol, it is $3.8 \times 10^4 \text{ dm}^3 \text{ mol}^{-1} \text{ s}^{-1}$.⁴⁷ These values are much higher than the equivalent reaction for water, which is $19 \text{ dm}^3 \text{ mol}^{-1} \text{ s}^{-1}$.⁴⁸

The dashed curve (c) in Figure 6 is obtained according to the following procedures. As is known, it is possible to obtain the time-dependent yield of the solvated electron from the yield measurements with the scavenging method. The general form of the empirical formula used to describe the influence of

scavenger reaction is

$$G(S) = G_{\text{esc}} + (G^\circ - G_{\text{esc}})F(S) \quad (16)$$

where $G(S)$ stands for the observed scavenged radiation chemical yield of a radical or molecular product at a given concentration of scavenger S , G° is the initial yield of the species, G_{esc} is the limiting yield of the species to escape spur reactions, and $F(S)$ is a semiempirical function describing the scavenging dependence.^{49,50} There are several semiempirical functions for $F(S)$; here, we use the one proposed by Warman et al.⁴⁹

$$F(S) = (a[S])^{1/2}/(1 + (a[S])^{1/2}) \quad (17)$$

where $[S]$ represents the solvated electron scavenger concentration and a is defined as the reactivity coefficient for the solvated electron. In the case of 12ED, the best fit of our experimental data gives: $G^\circ = 4.25 \times 10^{-7}$ mol/J, $G_{\text{esc}} = 7.05 \times 10^{-8}$ mol/J, and $a = 32.96$.

Then, the time-dependent yield of the solvated electron in 12ED can be obtained from the inverse Laplace transformation (ILT) of eq 16.⁵⁰ The numerical determination of the ILT gives the following equation in the units of moles per joule:

$$G(t) = 7.05 \times 10^{-8} + 3.5 \times 10^{-7} e^{(5.16 \times 10^7 t)} \operatorname{erfc}[(5.16 \times 10^7 t)^{1/2}] \quad (18)$$

Since the maximum scavenging power in the present study is 7.7 ns, we plot the curve of $G(t)$ (curve c) from 1 ns to 1 μ s. The $G(e_s^-)$ values at 200 ns are about 0.14 and 0.17 μ mol/J for the calculation and the experimental measurement.

Similarly, we can obtain the time-dependent yield of the solvated electron in 12PD and 13PD, as shown in Figure 6 (middle and bottom). In contrast to the case of 12ED, for these two solvents at picosecond time range, we do not observe any decay of the solvated electron. Moreover, the decay of the solvated electron in the nanosecond time range is faster in 12PD than in 13PD. In addition, we can deduce $G(e_s^-)$ at 100 ps, 0.35 and 0.38 μ mol J⁻¹, and $G(e_s^-)$ at 200 ns, 0.17 and 0.22 μ mol J⁻¹, for 12PD and 13PD, respectively (Table 1). We note that the dielectric constant and the viscosity of these two latter solvents are close but different from those of 12ED. For comparison, the data in water are also reported in Table 1.

Surprisingly, the yield calculations by ILT treatments of the scavenging data agree fairly well in the case of 13PD (Figure 6, bottom), in both picosecond and submicrosecond time ranges, whereas there are discrepancies between the time profiles measured in pulse radiolysis experiments and the time-dependent decays calculated for 12PD and 12ED. There are only a few data in the literature for the time measurements of the radiolytic yield in solvents from picosecond to microsecond. The same discrepancy had been reported for the hydrated electron.^{40,51} However, after a reanalysis of the available experimental data, Pimblott et al. found that the spatial distribution of secondary electrons produced in the energetic electron radiolysis of water should be nearly twice the width commonly used in previous modeling studies.⁵² Recently, a similar comparison has been done for time-dependent radiolytic yield of the solvated electron in THF, and at short times, an important difference has been found between the values obtained by scavenging methods and those directly measured with time-resolved spectroscopy.⁵³ Our present measurements also show that the two methods (direct and scavenging methods) are not equivalent for the radiolytic

yield determination. Equations 16–18 could be unreliable in the case of diols.

Conclusion

We have re-estimated the extinction coefficients at the maximum of the absorption bands of the solvated electron in 12ED, 12PD, and 13PD by conventional nanosecond pulse radiolysis. Given these extinction coefficients, we are able to describe the time dependence of the radiolytic yields of the solvated electron from picosecond to microsecond, using picosecond pulse radiolysis measurements. The radiolytic yield in these viscous solvents decreases much more rapidly than that in aqueous solutions within a few hundreds of nanoseconds after the pulse.

Acknowledgment. We are grateful to Mr. T. Ueda and Mr. K. Yoshii, and Prof. M. Uesaka for their technical assistance in experiments and encouragement. This work was partly entrusted by the Ministry of Education, Culture, Sports, Science and Technology (MEXT), Japanese Government, as a ‘‘Fundamental R&D program on water chemistry of supercritical pressure water under radiation field’’.

References and Notes

- Hart, E. J.; Boag, J. W. *J. Am. Chem. Soc.* **1962**, *84*, 4090–4095.
- Boag, J. W.; Hart, E. J. *Nature (London)* **1963**, *197*, 45–46.
- Keene, J. P. *Nature (London)* **1963**, *197*, 47.
- Hart, E. J.; Anbar, M. *The Hydrated Electron*; Wiley-Interscience: New York, 1970.
- Dorfman, L. M.; Jou, F. Y. *Ber. Bunsen-Ges.* **1971**, *75*, 681–685.
- Dorfman, L. M.; Jou, F. Y. Optical absorption spectrum of the solvated electron in ethers and in binary liquid systems. In *Electrons in Fluids*; Jortner, J., Kestner, N. R., Eds.; Springer: New York, 1972; pp 447–457.
- Ferradini, C.; Jay-Gerin, J. P. *Radiat. Phys. Chem.* **1996**, *48*, 473–480.
- Belloni, J.; Marignier, J. L. *Radiat. Phys. Chem.* **1989**, *34*, 157–171.
- Mostafavi, M.; Lin, M.; He, H.; Muroya, Y.; Katsumura, Y. *Chem. Phys. Lett.* **2004**, *384*, 52–55.
- Lampre, I.; Lin, M.; He, H.; Han, Z.; Mostafavi, M.; Katsumura, Y. *Chem. Phys. Lett.* **2005**, *402*, 192–196.
- Soroshian, B.; Lampre, I.; Pernot, B.; De Waele, V.; Pommeret, S.; Mostafavi, M. *Chem. Phys. Lett.* **2004**, *394*, 313–317.
- Soroshian, B.; Lampre, I.; Bonin, J.; Pernot, P.; Pommeret, S.; Mostafavi, M. *J. Phys. Chem. A* **2006**, *110*, 1705–1717.
- Bonin, J.; Lampre, I.; Pernot, P.; Mostafavi, M. To be published.
- Sauer, M. C.; Arai, S.; Dorfman, L. M. *J. Chem. Phys.* **1965**, *42*, 708–712.
- Arai, S.; Sauer, M. C. *J. Chem. Phys.* **1966**, *44*, 2297–2305.
- Okazaki, K.; Idriss-Ali, K. M.; Freeman, G. R. *Can. J. Chem.* **1984**, *62*, 2223–2229.
- Chandrasekhar, N.; Krebs, P. *J. Chem. Phys.* **2000**, *112*, 5910–5914.
- Jou, F. Y.; Freeman, G. R. *Can. J. Chem.* **1979**, *59*, 591–597.
- Brodsky, A. M.; Tsarevsky, A. V. *Inst. Elektrokhim.* **1975**, *222*, 1365–1368.
- Brodsky, A. M.; Tsarevsky, A. V. *J. Phys. Chem.* **1984**, *88*, 3790–3799.
- Jay-Gerin, J.-P.; Ferradini, C. *Radiat. Phys. Chem.* **1989**, *33*, 251–253.
- Jay-Gerin, J. P.; Ferradini, C. *J. Chim. Phys.* **1994**, *91*, 173–187.
- Muroya, Y.; Watanabe, T.; Wu, G.; Li, X.; Kobayashi, T.; Sugawara, J.; Ueda, T.; Yoshii, K.; Uesaka, M.; Katsumura, Y. *Radiat. Phys. Chem.* **2001**, *60*, 307–312.
- Muroya, Y.; Lin, M.; Watanabe, T.; Kobayashi, T.; Wu, G.; Ueda, T.; Yoshii, K.; Uesaka, M.; Katsumura, Y. *Nucl. Instrum. Methods Phys. Res., Sect. A* **2002**, *489*, 554–562.
- Muroya, Y.; Lin, M.; Iijima, H.; Ueda, T.; Katsumura, Y. *Res. Chem. Intermed.* **2005**, *31*, 261–272.
- Buxton, G. V.; Stuart, C. R. *J. Chem. Soc., Faraday Trans.* **1995**, *91*, 279–281.
- Muroya, Y.; Lin, M.; Wu, G.; Iijima, H.; Ueda, T.; Yoshii, K.; Uesaka, M.; Kudo, H.; Katsumura, Y. *Radiat. Phys. Chem.* **2005**, *72*, 169–172.

- (28) Elisei, F.; Mazzucato, U.; Görner, H.; Schulte-Frohlinde, D. *J. Photochem. Photobiol., A* **1989**, *50*, 209–219.
- (29) Simić, M.; Ebert, M. *Int. J. Radiat. Phys. Chem.* **1971**, *3*, 259.
- (30) Kihara, H.; Gondo, Y. *J. Raman. Spectrosc.* **1986**, *17*, 263–267.
- (31) Hiratsuka, H.; Sekiguchi, K.; Hatano, Y.; Tanizaki, Y.; Mori, Y. *Can. J. Chem.* **1987**, *65*, 1184–1189.
- (32) Solar, S. *J. Phys. Chem.* **1984**, *88*, 5624.
- (33) Poizat, O.; Buntinx, G.; Valat, P.; Wintgens, V.; Bridoux, M. *J. Phys. Chem.* **1993**, *97*, 5905.
- (34) Soroushian, B.; Lampre, I.; Belloni, J.; Mostafavi, M. *Radiat. Phys. Chem.* **2005**, *72*, 111–118.
- (35) Idriss-Ali, K. M.; Freeman, G. R. *Radiat. Phys. Chem.* **1984**, *23*, 89–96.
- (36) Wolff, R. K.; Bronskill, M. J.; Hunt, J. W. *J. Chem. Phys.* **1970**, *53*, 4211–4215.
- (37) Lam, K. Y.; Hunt, J. W. *Int. J. Radiat. Phys. Chem.* **1975**, *7*, 317.
- (38) Jonah, C. D.; Miller, J. R.; Matheson, M. S. *J. Phys. Chem.* **1977**, *81*, 1618–1622.
- (39) Lewis, M. A.; Jonah, C. D. *J. Phys. Chem.* **1986**, *90*, 5367–5372.
- (40) Hunt, J. W. Early events in radiation chemistry. In *Advances in Radiation Chemistry*; Burton, M., Magee, J. L., Eds.; John Wiley & Sons: New York, 1975; Vol. 5, pp 185–315.
- (41) Akhtar, S. M. S.; Freeman, G. R. *J. Phys. Chem.* **1971**, *75*, 2756–2762.
- (42) Jha, K. N.; Freeman, G. R. *J. Chem. Phys.* **1972**, *57*, 1408–1414.
- (43) Freeman, G. R. Radiation Chemistry of Ethanol: A review of the data on yields, reaction rate parameters, and spectral properties of transients. *NSRDS-NBS* **1974**, *48*, 10.
- (44) Ferradini, C.; Jay-Gerin, J. P. *Radiat. Phys. Chem.* **1996**, *48*, 473–480.
- (45) Johnson, D. W.; Salmon, G. A. *Radiat. Phys. Chem.* **1977**, *10*, 294–296.
- (46) Getoff, N.; Ritter, A.; Schwörer, F. *J. Chem. Soc., Faraday Trans. 1* **1983**, *79*, 2389–2404.
- (47) Han, Z.; Katsumura, Y.; Lin, M.; He, H.; Muroya, Y. *Chem. Phys. Lett.* **2005**, *404*, 267–271.
- (48) Buxton, G. V.; Greenstock, C. L.; Helman, W. P.; Ross, A. B. *J. Phys. Chem. Ref. Data* **1988**, *17*, 513.
- (49) Warman, J. M.; Asmus, K. D.; Schuler, R. H. *J. Phys. Chem.* **1969**, *73*, 931–939.
- (50) Laverne, J. A.; Pimblott, S. M. *J. Phys. Chem.* **1991**, *95*, 3196–3206.
- (51) Buxton, G. V. Radiation chemistry of the liquid state: (1) water and homogeneous aqueous solutions. In *Radiation Chemistry: Principles and Applications*. Eds. Farhataziz, Rodgers, M. A. J., Eds.; VCH Publishers: New York, 1987; p 343.
- (52) Pimblott, S. M.; LaVerne, J. A.; Bartels, D. M.; Jonah, C. D. *J. Phys. Chem.* **1996**, *100*, 9412–9415.
- (53) De Waele, V.; Sorgues, S.; Pernot, P.; Marignier, J. L.; Monard, H.; Larbre, J. P.; Mostafavi, M. *Chem. Phys. Lett.* **2006**, *423*, 30–34.